

Chain Rigidity of Substituted Aromatic Polyamides

W. R. Krigbaum,[†] T. Tanaka,[‡] G. Brelsford,^{*§} and A. Ciferri^{||}

Department of Chemistry, Duke University, Durham, North Carolina 27706,
 Unitika Ltd., 23 Koza Kura, Uji, Kyoto 611, Japan, Westvaco Research, North Charleston,
 South Carolina 29411-2905, and Instituto di Chimica Industriale, University of Genoa,
 16132 Genoa, Italy

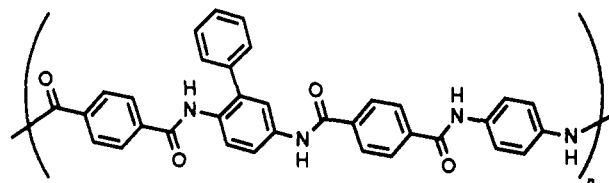
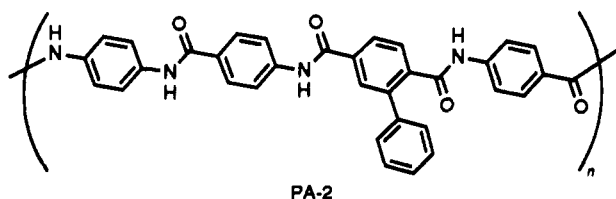
Received November 28, 1989; Revised Manuscript Received April 8, 1991

ABSTRACT: Static and dynamic light scattering and viscosity techniques were used for a dilute solution study of fractions of two aromatic polyamides having a phenyl substituent on every fourth ring. With respect to their unsubstituted analogues, poly(*p*-benzamide) (PBA) and poly(*p*-phenylenediamine-terephthalic acid) (PPTA) respectively, PA-2 and PA-4 show increased solubility in organic solvents and smaller persistence length, q . The average value of q for PA-2 in DMAC + 1% LiCl is 123 ± 52 Å, whereas for PBA q ranges from 240 to 750 Å. The average value of q for PA-4 in DMAC + 4% LiCl is 85 ± 26 Å, as opposed to a range from 150 to 290 Å for PPTA. We conclude that even one phenyl substituent on every four rings has a significant effect in making the chain more flexible. This occurs when substitution is either on the terephthalic acid or on the diamine moiety. The chains still retain the ability to form a mesophase in concentrated solutions.

Introduction

Bair et al.¹ attempted to increase the solubility of an aromatic polyamide in organic solvents by introduction of a chloro substituent on the *n*-phenylenediamine ring. They reacted the diacid chloride of terephthalic acid with 2-chloro-1,4-phenylenediamine forming polymers with inherent viscosity of 2.01 dL/g in H₂SO₄. They report a solubility of 12% in DMAC containing 5% LiCl. The patents of Payet² and Harris³ have disclosed that the introduction of a phenyl substituent in an A-A + B-B polyester is quite effective in lowering the melting temperature. Krigbaum et al.⁴ have compared the efficiency of various substituent groups on the benzene rings of the aromatic polyesters in depressing the crystal-nematic transition temperature. That study showed that a phenyl or cyclohexyl substituent is more effective in lowering the crystal-anisotropic transition temperature than a chloro substituent. Hence, we expected that a phenyl substituent would increase the solubility of an aromatic polyamide in organic solvents more than a chloro substituent. This expectation was confirmed by the behavior of several phenyl-substituted all-aromatic polyamides that we prepared using the phosphorylation reaction.⁵

In this paper we utilize light scattering and viscosity measurements to determine the persistence length of two members of the latter class having the repeating units



It should be noted that only one ring in four has a phenyl substituent and that substitution is on the terephthalic acid residue for PA-2 and on the diamine residue for PA-4. Moreover, apart from the substitution, PA-4 is similar to poly(*p*-phenylenediamine-terephthalic acid) (PPTA, the polymer forming the Kevlar fiber), whereas PA-2 is closer to, although not identical with, poly(*p*-benzamide) (PBA). Both PA-2 and PA-4 were found to be soluble in organic solvents such as *N,N*-dimethylacetamide (DMAC) containing 4% LiCl with solubility limits well above those of PBA and PPTA.⁵ The synthesis yielded polymers of fairly high molecular weight (inherent viscosity in 96% H₂SO₄ of 3.28 and 2.28 for PA-2 and PA-4, respectively).

The chain extension of semirigid polymers can be described by the persistence length, q , a parameter arising from the wormlike chain model of Kratky and Porod.⁶ If the contour length, L , of a chain is large compared to the persistence length, the chain conformation can be represented by the Kuhn chain model.⁷ In this limit the length of the Kuhn link, A , is twice the persistence length, $A = 2q$. Ermman et al.⁸ have calculated the lengths of the various units in our polyamide. According to their results, the projection length of the repeat units for PA-2 and PA-4 are approximately 26 Å in length. Since the weight of the repeating unit is 552 Da, the molecular weight per unit chain length is 21.2 Da/Å. Their calculation of the persistence length yielded ~430 Å for both PPTA and PBA. Larger values were obtained for the corresponding aromatic polyesters.⁸

Several papers have reported measurements of the persistence lengths of different aromatic polyamides, such as PPTA and PBA.⁹⁻¹³ The values range from 150 to 290 Å for PPTA in H₂SO₄ and 240 to 750 Å for PBA in DMAC + 3% LiCl or in H₂SO₄. In previous work we reported¹⁴

[†] Duke University.

[‡] Unitika Ltd.

^{*} Westvaco Research.

^{||} University of Genoa.

Table I
Viscosity Data

PA-2		PA-4	
fraction	$[\eta]$, ^a dL/g	fraction	$[\eta]$, ^b dL/g
1	7.45	1	3.70
2	7.30	2	2.64
3	7.12	3	2.24
4	5.88	4	2.11
5	5.55		
6	4.98		
7	4.80		
8	4.09		
9	3.27		
10	2.26		
11	1.31		

^a DMAC + 1% LiCl, 25 °C. ^b DMAC + 4% LiCl, 25 °C with previous exposure to 60 °C.

the persistence length of the polyester poly(phenyl *p*-phenylene terephthalate). The average value obtained was only 100 Å, indicating that the phenyl substituent on the hydroquinone ring makes the aromatic polyester chain more flexible.

Experimental Section

1. Materials. The polymer samples used in this investigation were prepared as previously described.⁵ PA-2 had an inherent viscosity (0.5% concentration at 25 °C) of 5.27 dL/g in DMAC containing 1 g/dL LiCl. PA-4 had $\eta_{inh} = 4.15$ dL/g in NMP + 4% LiCl. Fractionation of PA-2 was performed by dissolving 7 g of polymer in 5 L of DMAC + 1% LiCl. Seven fractions were obtained by successive precipitation by methanol addition at a constant temperature of 23 °C. The first fraction was rather large (2.5 g), so it was redissolved in 3 L of solvent and refractionated into five fractions. Each gel phase was precipitated by pouring it slowly into a Waring blender containing excess methanol. All 11 fractions were dried at 50 °C in a vacuum oven for several days. Fractionation of PA-4 was similarly performed starting from DMAC + 4% LiCl. DMAC was HPLC gold label grade and was used as received. LiCl content was invariably 1% for PA-2 and 4% for PA-4. Density, refractive index, and viscosity for the DMAC + 1% LiCl solvent (treated as a one-component diluent) at 25 °C were 0.9457 g/cm³, 1.435, and 1.21 cP, respectively. For the DMAC + 4% LiCl solvent the refractive index was 1.4504.

2. Physical Measurements. Viscosities were measured at 25 ± 0.1 °C (occasionally at 60 °C) on an Ubbelohde viscometer. Light scattering was performed at 25 °C. The light scattering instrument consisted of an automated Picker goniometer, an Inova 90-3 argon ion laser, and a Malvern Instruments RR109 detector containing an ITT FW130 photomultiplier tube and a narrow band-pass filter. A Glan-Thompson polarizer and analyzer determined the polarization of the incident and scattered light. The sample cell was cylindrical with a diameter of 1.6 cm. The sample cell was placed in a temperature-controlled vat containing xylenes, which also contained a beam stop. The reliable angular range was 20–130°. A 1-mm aperture was used for static measurements and a 0.5-mm aperture for the dynamic measurements. The experimental procedures have been described elsewhere.¹⁴ All experiments measure vertically or horizontally polarized light scattered from vertically polarized incident light. The refractive index increment was measured at five concentrations and $\lambda_0 = 436, 546,$ and 632.8 nm. For PA-2 dn/dc at $\lambda_0 = 514.5$ nm is 0.3478 mL/g. For PA-4, the value $dn/dc = 0.268$ mL/g measured at $\lambda_0 = 632.8$ nm was used.

Results and Discussion

1. Intrinsic Viscosities. $[\eta]$ of PA-2 and PA-4 fractions are collected in Table I. Linear plots of η_{sp}/c and $\ln \eta_{rel}/c$ allowed a reliable extrapolation of the reported $[\eta]$ values when the concentration was below 0.1 g/dL. At higher concentrations nonlinearity was evident. For PA-4 the temperature dependence of $[\eta]$ was investigated. The

highest molecular weight sample exhibited an increase of $[\eta]$ with temperature, which was slowly reversible upon cooling. In particular, $[\eta]$ increased from 3.20 to 3.70 dL/g between 25 and 60 °C. Usually $[\eta]$ for extended-chain polymers decreases with temperature, although a positive temperature coefficient was reported for PBA in DMAC + 3% LiCl.¹⁵ The present results suggest that a small degree of aggregation occurs in the selected solvents for the higher molecular weight samples and where concentrations exceed 0.1% (it will be recalled that the unsubstituted polymers PBA and PPTA are actually insoluble in the solvents we used for PA-2 and PA-4).¹⁵ To circumvent the problem, solutions in which some aggregation was suspected were exposed at 60 °C before making measurements at 25 °C.

2. Static Light Scattering. In this work toluene was used as a secondary intensity standard. The Rayleigh ratio for vertically polarized incident and scattered light is

$$R_{vv}(\theta) = (n_s/n_v)^2 [\Delta I/I_t(90^\circ)] R_{vv,t}(90^\circ) \sin(\theta) \quad (1)$$

where n_s and n_v are the refractive indices of the solvent and of the xylene in the vat, respectively. ΔI is the excess scattering of the solution at 90°, $I_t(90^\circ)$ is the scattered intensity of toluene at 90°, and $R_{vv,t}(90^\circ)$ is the Rayleigh ratio of toluene at 90°. We have assigned $R_{vv,t}(90^\circ)$ equal to 24.0×10^{-6} cm⁻¹ at 514.5 nm (PA-2) and 10.64×10^{-6} cm⁻¹ at 632.8 nm (PA-4) from a plot of literature data given by Brelford.¹⁶

The dependencies of scattering angle and concentration are given by the relation of Zimm:¹⁷

$$Kc/R_{vv}(\theta, c) = P^{-1}(\theta) [1/\langle M \rangle_w + 2A_2c] \quad (2)$$

where A_2 is the second virial coefficient and $K = 4\pi^2 n_s^2 (dn/dc)^2 / N_A \lambda_0^4$ and $P^{-1}(\theta) = 1 + (16\pi^2 n_s^2 / 3\lambda_0^2) \langle s^2 \rangle_z \sin^2(\theta/2)$. Here dn/dc is the refractive increment, N_A is Avogadro's number, λ_0 is the wavelength of light in a vacuum, $\langle M \rangle_w$ is the weight-average molecular weight, $\langle s^2 \rangle_z$ is the z-average radius of gyration of the polymer molecule, and θ is the scattering angle. The value of the optical constant was $K = 2.333 \times 10^{-6}$ mol cm²/g² for PA-2, and $K = 6.177 \times 10^{-7}$ mol cm²/g² for PA-4 (cf. Experimental Section). One obtains values of $\langle M \rangle_w$ and $\langle s^2 \rangle_z$ by plotting $Kc/R_{vv}(\theta, c)$ versus $\sin^2(\theta/2)$ and extrapolating to zero scattering angle and zero concentration. However, these are apparent values and must be corrected to their true values if the solute exhibits depolarization. The depolarization ratio in the limit of zero scattering angle and concentration is given by

$$\rho_v = R_{vh}/R_{vv} \quad (3)$$

where R_{vh} and R_{vv} are the Rayleigh ratios measured for horizontally and vertically polarized scattered light, respectively. This ratio is related to the total chain anisotropy δ by

$$\rho_v = \frac{3\delta^2}{5 + 4\delta^2} \quad (4)$$

where δ is a function of the number of chain scattering elements.

Corrections to apparent values, based on the theory of Nagai,¹⁸ are

$$\langle M \rangle_w = M_{app} / (1 + 4\delta^2/5) \quad (5)$$

$$\langle s^2 \rangle_z = \langle s^2 \rangle_{app} (1 + 4\delta^2/5) / (1 - 4f_1\delta/5 + 4(f_2\delta)^2/7) \quad (6)$$

$$A_2 = A_{2,app} (1 + 4\delta^2/5)^2 \quad (7)$$

Table II
Light Scattering Results

fraction	$10^{-3}\langle M \rangle_w$	$10^3 A_2$ (cm ³ g)/ mol	$10^{-4}\langle s^2 \rangle_z$, Å ²	$10^{-4}\langle s^2 \rangle_w$, Å ²	$10^2 \delta^2$	$\mu_2/\bar{\Gamma}^2$
Sample PA-2						
1	57.6	9.65	14.1	13.0	1.16	0.091
2	55.1	9.45	12.4	11.0	0.991	0.154
3	54.1	8.75	12.4	11.2	1.33	0.125
4	43.3	10.2	11.4	10.2	1.57	0.139
5	40.7	9.65	11.7	10.8	1.47	0.091
6	38.3	11.0	11.0	9.92	2.09	0.125
7	31.1	10.4	8.02	7.53	1.83	0.077
8	29.4	11.9	8.23	7.43	2.36	0.100
9	20.0	9.76	4.92	4.50	2.55	0.139
10	13.7	11.4	3.42	3.05	3.43	0.139
11	8.41	15.2	2.05	1.80	4.20	0.143
Sample PA-4						
1	42.4	6.01	9.02	6.01	2.00	
2	26.9	5.65	5.28	3.52	2.75	
3	25.0	5.16			2.30	
4	22.1	4.45			3.45	

where the apparent values of $\langle M \rangle_w$, $\langle s^2 \rangle_z$, and A_2 are obtained from eq 2. Corrected values of $\langle M \rangle_w$, A_2 , and $\langle s^2 \rangle_z$ are listed in Table II. f_1 and f_2 are functions of the number of persistence lengths in the chain and range between unity for rods and zero for coils. The values in Table II were calculated by using f_1 and f_2 equal to zero. Values of δ^2 may fluctuate due to differences in polydispersity between the fractions but still reveal the expected trend with molecular weight.

We also investigated a second procedure, also due to Nagai,¹⁸ which involves the relation

$$[R_{vv}(\theta) - (4/3)R_{vh}(\theta)]_{c=0} = Kc\langle M \rangle_w[1 - (\langle s^2 \rangle_z/3)k^2] \quad (8)$$

The quantity on the left is plotted against k^2 where k is the scattering wave vector magnitude $(4\pi n_s/\lambda_0) \sin(\theta/2)$. Corrected values of $\langle M \rangle_w$ and $\langle s^2 \rangle_z$ are obtained from the intercept and slope of this plot. This procedure gave nearly the same values of $\langle M \rangle_w$, but eq 8 gives values of the radius of gyration that are lower by 20% for lower molecular weights and by 30% for the higher molecular weights. Experimental uncertainty in $\langle s^2 \rangle_z$ from eq 2 is between 5 and 10%. Since we have no explanation for this difference, we rely instead on values of $\langle s^2 \rangle_z$ obtained from eq 2.

3. Dynamic Light Scattering. The diffusion coefficient can be obtained by measuring time-dependent fluctuations of the scattered light. The correlation function is given by

$$G(\tau) = \lim_{T \rightarrow \infty} \frac{1}{2T} \int_{-T}^{+T} I(t)I(t+\tau) dt \quad (9)$$

By taking the Fourier transform of eq 9 one obtains the correlation function. The relation given by Ford¹⁹ is

$$G(\tau) = 1 + 2f(n_{\text{coh}})(I_s/I_{\text{LO}}) \exp(-2Dk^2\tau) \quad (10)$$

where I_s is the intensity of the scattered light. I_{LO} is the intensity of the local oscillator, and $f(n_{\text{coh}})$ is a function of the number of coherence areas. For our spectrometer $f(n_{\text{coh}})$ is near unity since $n_{\text{coh}} = 0.0727$. If the scattering system is polydisperse, the correlation function is given by

$$G(\tau) = 1 + b \exp[-\bar{\Gamma} + \sum_i (-1)^i \mu_i \tau^i / i!] \quad (11)$$

where $\bar{\Gamma}$ is the average relaxation rate. The method of cumulants was used to determine the first ($\bar{\Gamma}$) and second

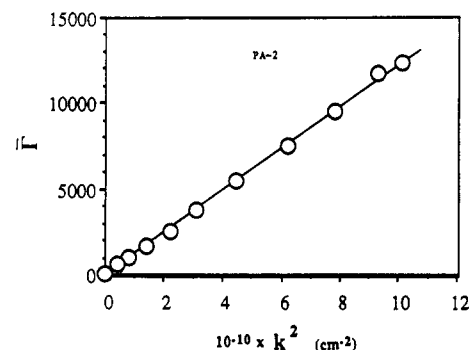


Figure 1. Average relaxation rate, $\bar{\Gamma}$, plotted against the square of the reciprocal lattice vector, k^2 , for PA-2.

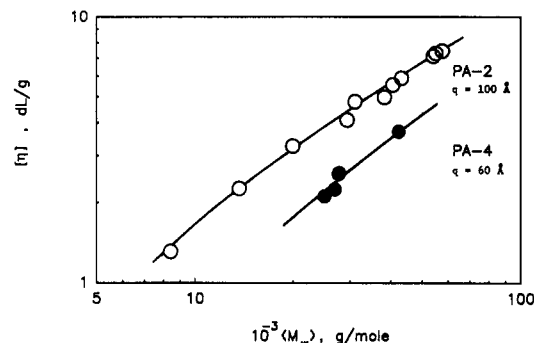


Figure 2. Fit of the intrinsic viscosity-molecular weight dependence to the treatment of Yamakawa and Fujii²⁰ for samples PA-2 and PA-4. $d = 7$ Å; $M_L = 21.2$ Da/Å.

(μ_2) cumulants from the experimental correlation functions. In order to evaluate the diffusion coefficient, one needs to be in the regime where $k\langle s^2 \rangle_z^{1/2} \ll 1$. In this case $\bar{\Gamma} = Dk^2$. We measured $\bar{\Gamma}$ for the highest molecular weight fraction of PA-2 over the angular range 20–130°. Figure 1 illustrates a plot of $\bar{\Gamma}$ versus k^2 . The data are well represented by a straight line passing through the origin, which indicates the $k\langle s^2 \rangle_z^{1/2} \ll 1$. For the other PA-2 fractions, we measured $\bar{\Gamma}$ at 30° to obtain diffusion coefficients.

4. Molecular Weight Dependencies and Persistence Length. Figure 2 illustrates a log-log plot of intrinsic viscosity versus the weight-average molecular weight. The Mark-Houwink equations are

$$\text{PA-2: } [\eta] = 5.78 \times 10^{-4} \langle M \rangle_w^{0.88} \quad (12a)$$

$$\text{PA-4: } [\eta] = 3.98 \times 10^{-4} \langle M \rangle_w^{0.86} \quad (12b)$$

We obtained a persistence length by fitting these data to the theory of Yamakawa and Fujii.²⁰ This plot is shown in Figure 2. The theoretical lines represent the equation²⁰

$$[\eta] = \frac{\Phi' L'^{3/2}}{\lambda^3 \langle M \rangle_w} \quad (13)$$

where $L' = \lambda \langle M \rangle_w / M_L$ is the reduced contour length, M_L is the mass per unit length, and $\lambda = (2q)^{-1}$. Φ' is a function of L' and of the reduced diameter d' ($=\lambda d$) calculated by Yamakawa and Fujii. Persistence lengths of approximately 100 and 60 Å are indicated respectively for PA-2 and PA-4, assuming a chain diameter of 7 Å.

Alternatively, q was obtained by using the Bohdanecky²¹ treatment, which involves the equation

$$(\langle M \rangle_w^2 / [\eta])^{1/3} = A + B \langle M \rangle_w^{1/2} \quad (14)$$

where $A = A_0 M_L \Phi_\infty^{-1/3}$ and $B = 1.05 \Phi_\infty^{-1/3} (2q/M_L)^{-1/2}$. A_0

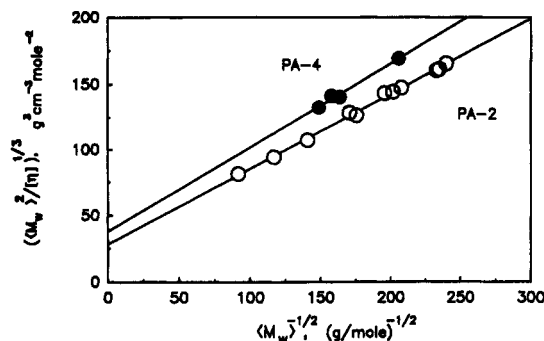


Figure 3. Intrinsic viscosity data plotted according to the treatment of Bohdanecky²¹ for samples PA-2 and PA-4.

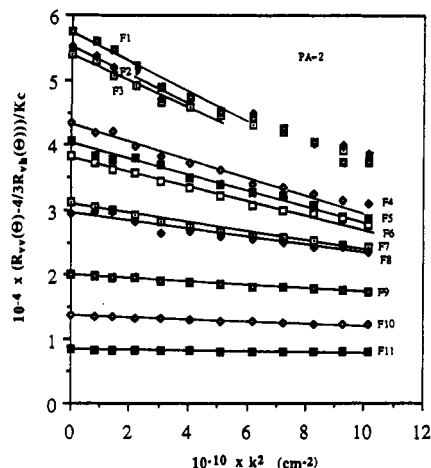


Figure 4. Plot of the anisotropy factor shown in the left-hand side of eq 15 versus k^2 for all 11 fractions of sample PA-2.

is a function of d' given by Bohdanecky and Φ_∞ is the limiting value of Φ ($\Phi_\infty = 2.86 \times 10^{23}$) for nondraining coils in the limit of infinite molecular weight. The solid lines in Figure 3 are linear least-square fits to the data for PA-4 and PA-2 according to eq 14. Using $M_L = 21.2 \text{ Å}^{-1}$ and slopes 0.57 and 0.64, respectively, we calculate $q = 83 \text{ Å}$ for PA-2 and $q = 66 \text{ Å}$ for PA-4. From the intercept (38.0) for PA-4, $q = 66 \text{ Å}$ and Bohdanecky's relation for A_0 , we estimate a chain diameter of 6 Å.

The evaluation of the persistence length using the light scattering data may be done by a method developed by Ying and Chu:²²

$$[R_{vv}(\theta) - (4/3)R_{vh}(\theta)]/Kc = \langle M \rangle_w [1 - (qL/9)\{1 - (3/X) - (4\epsilon/15X)\}k^2] \quad (15)$$

where $X = L/q$, L being the contour length, K is the optical constant, and k is the magnitude of the scattering vector. If the left-hand side of eq 15 is plotted against k^2 , as shown in Figure 5 for each PA-2 fraction, the ratio of each slope to its corresponding intercept is obtained. The ratio for each fraction is plotted against L to derive q by

$$(\text{slope}/\langle M \rangle_w) = qL/9 - (q^2/9)[3 + (4/5)\delta_0] \quad (16)$$

where ϵ has been replaced by $3\delta_0$ (δ_0 being the intrinsic anisotropy of the scattering element given by Horn²³). Equation 16 can be rewritten in the following form:

$$y = qL/9 - y_0 \quad (17)$$

$$y_0 = (q^2/9)[3 + (4/5)\delta_0] \quad (18)$$

Figure 5 illustrates a plot of y versus L , for eleven PA-2 fractions. We deduce $q \sim 150 \text{ Å}$ from the slope of the line (~ 16.7) within the linear portion of the plot. Unfortu-

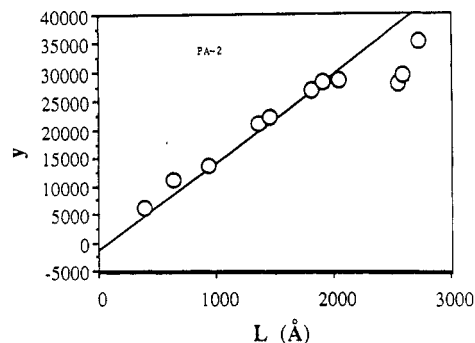


Figure 5. Function y plotted against L according to eqs 17 and 18 due to Ying and Chu²² for PA-2.

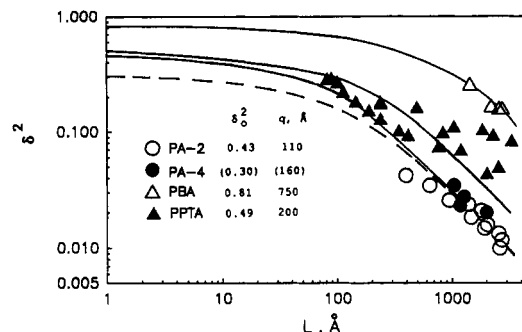


Figure 6. Plot of molecular anisotropy for wormlike chains against L for PA-2, PA-4, and literature results for PPTA^{9,13} and PBA.¹³ Values of q and δ_0 used to calculate the solid curves with eq 19 are attached.

nately, the estimate of δ_0 from the intercept ($y_0 \sim -1800$) with $q = 150 \text{ Å}$ yields an unphysical result ($\delta_0 = -2.85$) since the range defined for δ_0 is between 1 and $-1/2$.²³ The result for δ_0 may be due to uncertainty in extrapolating excess depolarized scattered light to the zero angle, infinite dilution limit in combination with the Ying-Chu plot.

The method of Arpin and Strazielle⁹ provides an alternative comparison using depolarized scattering data. Their result for a wormlike chains is

$$\delta^2 = \delta_0^2 \left\{ \frac{2}{x} - \frac{2}{x^2} (1 - \exp(-x)) \right\} \quad (19)$$

where x equals $3L/q$. Figure 6 shows a plot of δ^2 against L for PA-2 and PA-4. For comparison, we have included literature results for PBA¹³ and PPTA.^{9,13} The solid curve through PBA data was calculated by using $q = 750 \text{ Å}$ and $\delta_0^2 = 0.81$.¹³ The curve through the PPTA data was calculated by using $q = 200 \text{ Å}$ and $\delta_0^2 = 0.49$.⁹ We note that the authors of ref 24 conclude that the values of q for PBA and PPTA are much smaller. This conclusion was based on data in a range of M_w where q is insensitive to δ .

The solid curve through the phenyl-substituted polyamides was calculated with eq 19 using $q = 110 \text{ Å}$, $M_L = 21.2 \text{ Å}^{-1}$, and a δ_0^2 value equal to 0.43. This value of δ_0^2 is equivalent to the value measured for benzanilide by Zero and Aharoni²⁴ in a study of monodisperse aromatic polyamide oligomers. With this value of δ_0^2 we find that the value of q ($=110 \text{ Å}$) required to fit the trend in Figure 6 is somewhat smaller than the value deduced for PA-2 in Figure 5. Due to the phenyl substituents, we arbitrarily chose a lower δ_0^2 value ($=0.30$) and found that a reasonable fit to the data is obtained with $q = 160 \text{ Å}$ (dashed curve). In either case, it is clear that the phenyl-substituted polymers are less chain extended in their respective solvents compared to the unsubstituted polyamides.

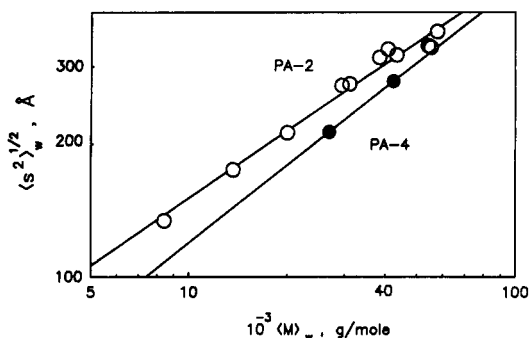


Figure 7. log-log plot of the mean-square radius of gyration, $\langle s^2 \rangle_w^{1/2}$ versus $\langle M \rangle_w$ for samples PA-2 and PA-4.

To proceed with the radius of gyration data, we estimate a correction of $\langle s^2 \rangle_z$ values to their weight-average values, $\langle s^2 \rangle_w$. For sample PA-2 (for which a more thorough fractionation was performed) we assume that the molecular weight distribution of our fractions can be represented adequately by the Schultz-Zimm distribution.²⁵ We approximate the width of the distributions by

$$\frac{\mu_2}{\bar{I}^2} \approx \frac{\langle M \rangle_w}{\langle M \rangle_n} - 1 = h^{-1} \quad (20)$$

where μ_2/\bar{I}^2 are the normalized second cumulants extrapolated to infinite dilution for PA-2 fractions given in column 7 of Table II. Values of $\langle s^2 \rangle_w$ calculated in this way using

$$\frac{\langle s^2 \rangle_z}{\langle s^2 \rangle_w} = \frac{h+2}{h+1} \quad (21)$$

and the dynamic light scattering data are found in column 5 of Table II. For sample PA-4, the correction for polydispersity was estimated by assuming the Schultz-Zimm distribution and $\langle M \rangle_w/\langle M \rangle_n = 2$. Results are included in the fifth column of Table II.

Figure 7 illustrates a log-log plot of $\langle s^2 \rangle_w^{1/2}$ versus $\langle M \rangle_w$. The equations are

$$\text{PA-2: } \langle s^2 \rangle_w^{1/2} = 1.41 \langle M \rangle_w^{0.507} \quad (22a)$$

$$\text{PA-4: } \langle s^2 \rangle_w^{1/2} = 0.481 \langle M \rangle_w^{0.585} \quad (22b)$$

The molecular weight exponent is smaller than we would have expected, since it is similar in magnitude to that of random flight chains (the exponent was 0.78 in the case of PPTA).¹³ This observation may be an artifact of the fractionation performed and the approximation used to correct the data to a common average.

Benoit and Doty²⁶ have given the following relation for the radius of gyration of a wormlike chain:

$$\langle s^2 \rangle_w = \frac{Lq}{3} - q^2 + \frac{2q^3}{L} - \frac{2q^4}{L^2} [1 - \exp(-L/q)] \quad (23)$$

Figure 8 shows a plot of $\langle s^2 \rangle_w/\langle M \rangle_w$ versus L . The fit of eq 23 is not particularly good for PA-2. It appears that the persistence length would be approximately 200 Å from the trend of this plot at the highest molecular weights. Both data points for PA-4 fall on the curve for $q = 105$ Å. By comparison, if we assume that the highest molar mass fractions for both polymers have reached the coil limit, we find that q is 144 Å for PA-2 (fraction 1) and 90 Å for PA-4 (fraction 1) using the relation $q = 3\langle s^2 \rangle_w M_L / \langle M \rangle_w$.

Turning now to the translational diffusion coefficient, it is important that the concentrations used are below that

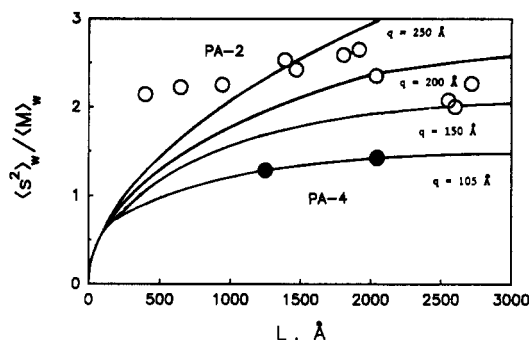


Figure 8. Plot of $\langle s^2 \rangle_w/\langle M \rangle_w$ versus the chain contour length, L , compared with values calculated according to the Benoit-Doty²⁶ equation for the wormlike chain. Data for samples PA-2 and PA-4.

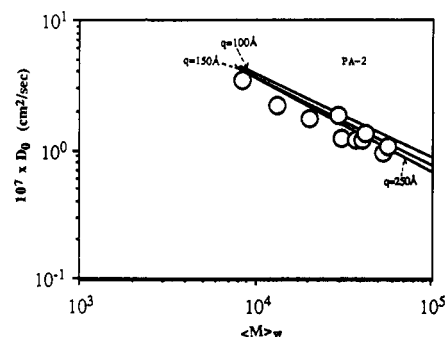


Figure 9. Attempt to fit the molecular weight dependence of diffusion coefficients to the treatment of Yamakawa and Fujii²⁹ for PA-2.

at which the polymer molecules begin to overlap. Ying and Chu²⁷ have given the following relation for the critical concentration of a wormlike chain:

$$c^* = 2^{3/2} \langle M \rangle_w / [N_A (qL)^{3/2}] \quad (24)$$

We took $q = 150$ Å in order to estimate c^* . The translational diffusion constant, D , was measured at several concentrations, all of which were below the estimated value of c^* . The concentration dependence of D is expressed as

$$D = D_0(1 + k_D c) \quad (25)$$

In all cases k_D was positive, as would be expected for a polymer in a good solvent.²⁸ Figure 9 illustrates a plot of D_0 versus $\langle M \rangle_w$. The molecular weight dependence is given by

$$D_0 \text{ (cm}^2/\text{s)} = 1.059 \times 10^{-4} \langle M \rangle_w^{-0.634} \quad (26)$$

We attempted to fit these data using the theory of Yamakawa and Fujii with $d = 7$ Å and $M_L = 21.2$ Å⁻¹.²⁹ The plot shown in Figure 9 does not lead to a precise value for the persistence length. We note evidence of extended chain behavior, however, since recent data for an aromatic polyamide hydrazide with a persistence length on the order of 100 Å exhibited a similar exponent (−0.62) for its D_0 versus $\langle M \rangle_w$ relationship.³⁰ The exponents for PPTA in H₂SO₄ and PBA in DMAC + 3% LiCl are −0.77 and −0.89, respectively.^{12,13}

Concluding Remarks

Persistence lengths obtained by various methods are summarized in Table III. A scatter by a factor of 2 between viscosity and light scattering (coil limit) has been often noticed and is discussed elsewhere.³² Average values for PA-2 and PA-4 are at least a factor of 2 smaller than the averages for PBA and PPTA discussed in the Introduction.

Table III
Values of the Persistence Length

data	method	q, Å	
		PA-2	PA-4
[η], $\langle M \rangle_w$	Yamakawa-Fujii	100	60
	Bohdanecký	83	66
anisotropy $\langle s^2 \rangle_w$, $\langle M \rangle_w$	Arpin et al.	110	110
	Benoit-Doty (or coil limit)	~200 (144)	105 (90)
average		123 \pm 52	85 \pm 26

The other noticeable effect of substitution is the increased solubility in organic solvents since PBA would not appreciably dissolve in DMAC with only 1% LiCl, nor would PPTA dissolve in DMAC + 4% LiCl.¹⁵ In fact, the solubility of PA-2 and PA-4 in the selected solvents is so large⁵ that the critical concentration C_p for mesophase formation¹⁵ can be attained. Preliminary results³¹ suggest that C_p for PA-2 is ~12% (twice the value for PBA¹⁵) and that fibers can be spun from the mesophase. In the case of PA-4, there is definite evidence that DMAC + 4% LiCl is not as good a solvent as DMAC + 1% LiCl is for PA-2. A small degree of aggregation may occur in solution, and the virial coefficient for PA-4/DMAC + 4% LiCl is much smaller than for the PA-2/DMAC + 1% LiCl system. Early crystallization may therefore encroach upon mesophase formation.³³

Increased solubility alone would be consistent with a randomness introduced by the (internal) copolymer effect. This effect was also observed in nitro-substituted polyamides.³⁴ However, the body of results clearly reveals an increased chain flexibility due to substitution. Examination of space-filling models indicates that the phenyl substituent, particularly on terephthalic acid, will force the neighboring carbonyl group out of the plane of the ring. This reduces the conjugation of the amide group with the aromatic ring and increases chain flexibility. In a similar view, the Harris patent³ discloses that the polyester of phenylterephthalic acid and hydroquinone has a lower melting temperature than the corresponding polyester of terephthalic acid and phenylhydroquinone,² both temperatures being substantially below that of the unsubstituted polyester.

Acknowledgment. We express our appreciation to the National Science Foundation for support of this project from Grant DMR-8419803. We also thank Unitika Ltd. for a stipend that supported T.T. during the course of this work at Duke University. G.B. thanks the C.N.R. of Italy

for support, enabling him to perform part of the work at the University of Genoa.

References and Notes

- (1) Bair, T. L.; Morgan, P. W.; Killian, F. L. *Macromolecules* **1977**, *10*, 1396.
- (2) Payet, C. R. U.S. Patent 4,159,365, 1979.
- (3) Harris, J. F., Jr. U.S. Patent 4,294,955, 1981.
- (4) Krigbaum, W. R.; Hakemi, H.; Kotek, R. *Macromolecules* **1985**, *18*, 965.
- (5) Krigbaum, W. R.; Preston, J.; Jadhav, J. Y. *Macromolecules* **1988**, *21*, 538.
- (6) Kratky, O.; Porod, G. *Recl. Trav. Chim.* **1949**, *68*, 1106.
- (7) Kuhn, W. *Kolloid Z.* **1936**, *76*, 2586; **1939**, *87*, 3.
- (8) Erman, B.; Flory, P. J.; Hummel, J. P. *Macromolecules* **1980**, *13*, 484.
- (9) Arpin, M.; Strazielle, C. *Macromol. Chem.* **1976**, *177*, 581; *Polymer* **1977**, *18*, 262.
- (10) Schaeffgen, J. R.; Foldi, V. S.; Logolla, F. M.; Good, V. H.; Gulrich, L. W.; Killian, F. L. *Polym. Prepr. (Am. Chem. Soc., Div. Polym. Chem.)* **1976**, *17*, 69.
- (11) Tsvetkov, V. N.; Shtennikova, I. N. *Macromolecules* **1978**, *11*, 306.
- (12) Ying, Q.; Chu, B.; Qian, R.; Bao, J.; Zhang, J.; Xu, C. *Polymer* **1985**, *26*, 1401.
- (13) Ying, Q.; Chu, B. *Macromolecules* **1987**, *20*, 871; *Makromol. Chem., Rapid Commun.* **1984**, *5*, 785; *Macromolecules* **1986**, *19*, 1580.
- (14) Krigbaum, W. R.; Tanaka, T. *Macromolecules* **1988**, *21*, 743.
- (15) Balbi, G.; Bianchi, E.; Ciferri, A.; Tealdi, A.; Krigbaum, W. R. *J. Polym. Sci., Polym. Phys. Ed.* **1980**, *18*, 2037.
- (16) Brelsford, G. L. Static and Dynamic Light Scattering Studies of Poly(terephthaloyl-4-aminobenzhydrazide) in Dimethyl Sulfoxide. Ph.D. Dissertation, Duke University, 1987.
- (17) Zimm, B. H. *J. Chem. Phys.* **1948**, *16*, 1099.
- (18) Nagai, K. *Polym. J.* **1972**, *3*, 67.
- (19) Ford, N. C. In *Dynamic Light Scattering*; Pecora, R., Ed.; Plenum: New York, 1971; Chapter 2.
- (20) Yamakawa, H.; Fujii, M. *Macromolecules* **1974**, *7*, 128.
- (21) Bohdanecký, M. *Macromolecules* **1983**, *16*, 1483.
- (22) Ying, Q.; Chu, B. *Makromol. Chem., Rapid Commun.* **1985**, *5*, 938.
- (23) Horn, P. *Ann. Phys.* **1955**, *10*, 386.
- (24) Zero, K.; Aharoni, S. M. *Macromolecules* **1987**, *20*, 1957.
- (25) Schulz, G. V. *Z. Phys. Chem. Abt. B* **1939**, *43*, 25.
- (26) Benoit, H.; Doty, P. *J. Phys. Chem.* **1953**, *57*, 958.
- (27) Ying, Q.; Chu, B. *Macromolecules* **1987**, *20*, 362.
- (28) Han, C. C. In *Dynamics Light Scattering*; Pecora, R., Ed.; Plenum: New York, 1986; Chapter 5.
- (29) Yamakawa, H.; Fujii, M. *Macromolecules* **1973**, *6*, 497.
- (30) Krigbaum, W. R.; Brelsford, G. *Macromolecules* **1988**, *21*, 2502.
- (31) Marsano, E., personal communication.
- (32) Ciferri, A. In *Developments in Oriented Polymers-2*; Ward, I. M., Ed.; Elsevier Affl. Science: London, 1989.
- (33) Brelsford, G. L.; Krigbaum, W. R. In *Liquid Crystallinity in Polymers*; Ciferri, A., Ed.; VCH Publishers: New York, 1991.
- (34) Aharoni, S. A. *Macromolecules* **1987**, *20*, 2010.

Registry No. PA-2, 133815-82-4; PA-4, 133815-83-5.